Cell Tissue Res (2016) 365:247–264
DOI 10.1007/s00441-016-2401-2

REGULAR ARTICLE

Differential patterns of histone methylase EHMT2 and its catalyzed histone modifications H3K9me1 and H3K9me2 during maturation of central auditory system

Lena Ebbers[1] · **Karen Runge**[1] · **Hans Gerd Nothwang**[1,2]

Received: 2 October 2015 / Accepted: 24 March 2016 / Published online: 15 April 2016

Abstract Histone methylation is an important epigenetic mark leading to changes in DNA accessibility and transcription. Here, we investigate immunoreactivity against the euchromatic histone-lysine N-methyltransferase EHMT2 and its catalyzed mono- and dimethylation marks at histone 3 lysine 9 (H3K9me1 and H3K9me2) during postnatal differentiation of the mouse central auditory system. In the brainstem, expression of EHMT2 was high in the first postnatal week and down-regulated thereafter. In contrast, immunoreactivity in the auditory cortex (AC) remained high during the first year of life. This difference might be related to distinct demands for adult plasticity. Analyses of two deaf mouse models, namely *Cldn14*$^{-/-}$ and *Cacna1d*$^{-/-}$, demonstrated that sound-driven or spontaneous activity had no influence on EHMT2 immunoreactivity. The methylation marks H3K9me1 and H3K9me2 were high throughout the auditory system up to 1 year. Young auditory neurons showed immunoreactivity against both methylations at similar intensities, whereas many mature neurons showed stronger labeling for either H3K9me1 or H3K9me2. These differences were only poorly correlated with cell types. To identify methyltransferases contributing to the persistent H3K9me1 and H3K9me2 marks in the adult brainstem, EHMT1 and the retinoblastoma-interacting zinc-finger protein RIZ1 were analyzed. Both were down-regulated during brainstem development, similar to EHMT2. Contrary to EHMT2, EHMT1 was also down-regulated in adult cortical areas. Together, our data reveal a marked difference in EHMT2 levels between mature brainstem and cortical areas and a decoupling between EHMT2 abundance and histone 3 lysine 9 methylations during brainstem differentiation. Furthermore, EHMT1 and EHMT2 are differentially expressed in cortical areas.

Keywords Deafness · Development · Epigenetics · Nervous system · Plasticity

This work was supported by the DFG priority program 1608 "Ultrafast and temporally precise information processing: normal and dysfunctional hearing" No428/10-1, No428/7-1 and the Cluster of Excellence Hearing4All to H.G.N.

✉ Hans Gerd Nothwang
hans.g.nothwang@uni-oldenburg.de

[1] Neurogenetics Group, Center of Excellence Hearing4All, School of Medicine and Health Sciences, Carl von Ossietzky University Oldenburg, 26111 Oldenburg, Germany

[2] Research Center for Neurosensory Science, Carl von Ossietzky University Oldenburg, 26111 Oldenburg, Germany

Introduction

During development, neurons acquire distinct fates despite sharing identical DNA sequences. These differentiation processes are controlled by epigenetic mechanisms (Goldberg et al. 2007; Lister et al. 2013; Sweatt 2013). Historically, the term epigenetics described the "causal mechanisms" by which "genes of the genotype bring about phenotypic effects" (Waddington 1942). The currently established epigenetic toolkit mainly comprises dynamic modifications of DNA and histones (Sweatt 2013; Yao and Jin 2014). At the DNA level, cytosine methylation is a core mechanism, whereas at the histone level, posttranslational modifications include methylation, acetylation, phosphorylation and monoubiquitination (Sweatt 2013).

Recently, the euchromatic histone-lysine N-methyltransferase 2 (EHMT2, a.k.a. G9a) has attracted much attention in neuro-epigenetics. EHMT2 is the dominant enzyme for the mono- and dimethylation of lysine 9 on histone 3 (H3K9me1 and H3k9me2, respectively; Shinkai and Tachibana 2011;

Fig. 1). H3K9me1 is often correlated with gene activation, whereas H3K9me2 is predominant in silenced genes (Barski et al. 2007). *Ehmt2*-knockout mice show high lethality during early embryonic development between embryonic days 9.5 and 12.5 and a remarkable growth retardation attributable to increased cell death (Tachibana et al. 2002). In addition, embryonic stem cells of these mice present severe differentiation defects (Tachibana et al. 2002).

In the nervous system, postnatal conditional inactivation of *Ehmt2* by a *Camk2a-Cre* driver mouse line in various forebrain areas results in de-repression of early neuronal progenitor and non-neuronal genes, suggesting a role of EHMT2 in the maintenance of neuron-specific transcriptional homeostasis (Schaefer et al. 2009). These transcriptional changes are associated with complex behavioral abnormalities such as diminished locomotion and exploration (Schaefer et al. 2009). EHMT2 is also critically involved in regulating neuronal gene expression in response to drugs (Maze et al. 2010). Finally, in *Drosophila*, EHMT is essential in dendritic plasticity, non-associative memory formation and consolidation or retrieval of new memories (Kramer et al. 2011). Outside the brain, interaction of EHMT2 with mediator and the neuron restrictive silencing factor REST represses neuronal genes (Ding et al. 2008; Roopra et al. 2004). Furthermore, the enzyme represses differentiation in adipocytes (Wang et al. 2013), skeletal muscle precursor cells (Ling et al. 2012) and T cells (Antignano et al. 2014). Together, these data suggest that EHMT2 mediates the epigenetic silencing of non-specific gene loci during lineage differentiation and holds an important position at critical developmental transitions and during the cellular response to external factors (Kramer 2016).

We therefore set out to investigate its expression in mice during the postnatal development of major centers of the ascending auditory pathway. During this period, these neurons undergo extensive changes in gene expression (Ehmann et al. 2013; Harris et al. 2005), abruptly alter their sensitivity to deafferentiation (Harris et al. 2008; Mostafapour et al. 2000) and undergo morphological and functional maturation (Friauf 2004; Kandler et al. 2009; Rubel et al. 2004; Yu and Goodrich 2014). As epigenetic markers are sensitive to external factors, we also probed the dependence of EHMT2 on sensory activity by analyzing its immunoreactivity in deaf mice.

In the course of our analysis, we observed a remarkable down-regulation of EHMT2 in the brainstem around hearing-onset but persisting H3K9 methylations. We thus included other H3K9 methyltransferases. The euchromatic histone-lysine N-methyltransferase 1 (EHMT1, a.k.a. GLP) is closely related to EHMT2 and shows the same substrate specificity in vitro (Ogawa et al. 2002; Tachibana et al. 2005; Weiss et al. 2010; Fig. 1). EHMT1 and EHMT2 form functional heteromeric complexes and a knockout of *Ehmt1* closely resembles the phenotype observed in *Ehmt2* deficiency (Schaefer et al. 2009; Tachibana et al. 2005). In humans, mutations in the methyltransferase *EHMT1* lead to Kleefstra syndrome characterized by mental retardation, facial dysmorphism, heart defects and hearing loss (Kleefstra et al. 2005). Additionally, we analyzed the retinoblastoma-interacting zinc-finger protein 1 (RIZ1, a.k.a. PRDM2), which preferentially monomethylates H3K9 (Congdon et al. 2014; Fig. 1).

Methods

Animals The experiments were performed on wild-type mice of the C57BL/6 strain, on *Cldn14*$^{-/-}$ mice lacking the tight junction protein claudin 14 (Ben-Yosef et al. 2003), on *Cacna1d*$^{-/-}$ mice lacking the L-type Ca^{2+}-channel $Ca_v1.3$ (Platzer et al. 2000) and on *Ptf1a:: Cre* (Kawaguchi et al. 2002) and *Atoh7:: Cre* (Yang et al. 2003) driver mouse lines, crossed to the tdTomato reporter line (Madisen et al. 2010;

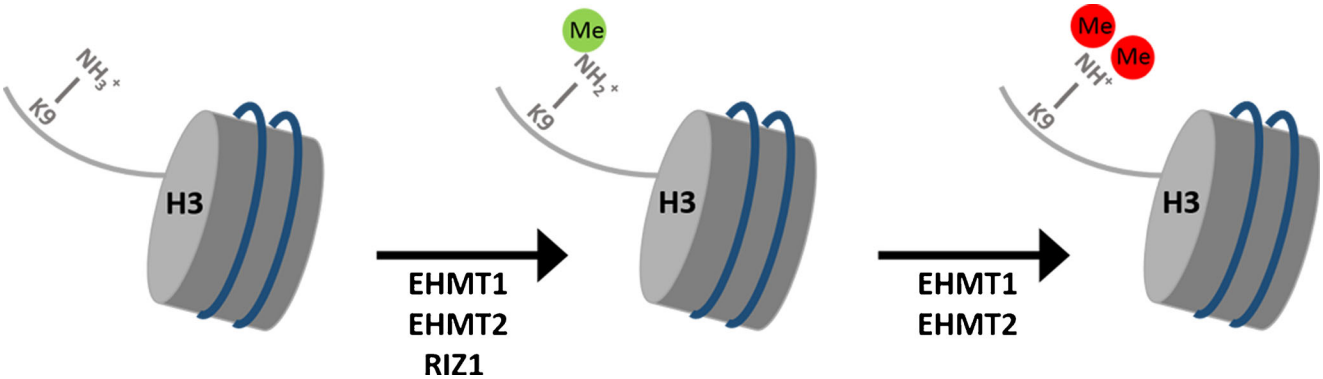

Fig. 1 Representation of euchromatic histone-lysine N-methyltransferase 1 (*EHMT1*), euchromatic histone-lysine N-methyltransferase 2 (*EHMT2*) and retinoblastoma-interacting zinc-finger protein 1 (*RIZ1*) action on histone 3 (*H3*). EHMT1 and EHMT2 are able to catalyze the addition of one or two methyl groups to lysine 9 of histone 3, whereas RIZ1 preferentially introduces monomethylation. Color coding of monomethylation (*green*) and dimethylation (*red*) also corresponds to the colors in Figs. 9, 10

tdTomato^{Ptf1a} and *tdTomato*^{Atoh7} mice, respectively) to visualize Ptf1a^{+} or Atoh7^{+} cell lineages. Table 1 provides an overview of the five different mouse lines and the number of animals that we studied. In total, 60 mice of both sexes were used. The day of birth was taken as postnatal day (P) 0. All protocols were in accordance with the German Animal Protection Law, were approved by the local animal care and use committee (LAVES Oldenburg) and followed the NIH guide for the care and use of laboratory animals.

Tissue processing Animals were transcardially perfused with Zamboni's fixative solution (15 % picric acid, 2 % paraformaldehyde in phosphate-buffered saline [PBS], pH 7.4) and brains were stored in 30 % sucrose in PBS until being sliced. Frozen sections (15 μm thick) were cut on a CM-1950 Cryostat (Leica, Wetzlar, Germany) or with a sliding microtome Microm HM 430 (Thermo Fisher Scientific, Waltham, Mass., USA) and mounted on Superfrost Plus microscope slides (Thermo Fisher Scientific).

Immunohistochemistry Slices were subjected to a standard antigen retrieval procedure with 10 mM trisodium citrate buffer (pH 6). Primary antibodies were diluted in carrier solution (1 % bovine serum albumin, 1 % goat serum and 0.3 % Triton X-100 in PBS, pH 7.4) and incubated overnight at 7 °C. To avoid denaturation of tdTomato in sections from transgenic *tdTomato*^{Ptf1a} and *tdTomato*^{Atoh7} mice, antigen retrieval was omitted for brain sections from these mouse lines. In this study, the following primary antibodies were used: mouse anti-EHMT1 (1:200; ab41969, Abcam, Cambridge, UK), rabbit anti-EHMT2 (1:500; HPA050550, Sigma-Aldrich, St. Louis, Mo., USA), rabbit anti-RIZ1 (1:200; HPA005809, Sigma-Aldrich), rabbit anti-histone H3 monomethyl lysine 9 (H3K9me1; 1:500; ab9045, Abcam) and mouse anti-histone H3 dimethyl lysine 9 (H3K9me2; 1:500; ab1220, Abcam). Specificity of antibodies used was given by analyses of the manufacturer: anti-EHMT1 gave no signal on ES cells of Ehmt1-knockout mice. Sigma prestige antibodies anti-EHMT2 and anti-RIZ1 were tested by immunohistochemistry against hundreds of normal and diseased tissues in the human protein atlas (http://www.proteinatlas.org); anti-H3K9me1 only showed slight cross-reactivity with H3K27me1 as revealed by immunoblot; the specificity of anti-H3K9me2 was tested in an enzyme-linked immunosorbent assay in which no binding to other methylated H3 peptides was observed. Binding was visualized by using Alexa-Fluor-coupled secondary antibodies (1:1,000; Invitrogen, Carlsbad, Calif., USA). These antibodies gave no signals on brain sections without prior incubation with primary antibodies. Slides were mounted with self-made embedding medium containing 4,6-diamidino-2-phenylindole (DAPI) to stain the nucleus.

Image acquisition and processing Images were taken with a BZ 8100 E fluorescence microscope (Keyence, Neu-Isenburg, Germany) or with a TCS SP8 confocal microscope (Leica, Wetzlar, Germany). Files were obtained by using the Keyence BZ observation software or Leica application suite X, respectively and processed in Adobe Photoshop CS6 (Adobe Systems, San José, Calif., USA) or Image J (U. S. National Institutes of Health, Bethesda, Md., USA).

Analysis by quantitative reverse transcription polymerase chain reaction Brainstem and neocortical tissues from two animals per age group were dissected and stored at −80 °C until being further processed. Total RNA from these tissues was isolated separately for each animal by using the innuPREP RNA Mini Kit (Analytik Jena, Jena, Germany) and transcribed into cDNA following the instructions of the RevertAid RT reverse transcription kit (Fermentas, Waltham, Mass., USA). Reverse transcription quantitative polymerase chain reaction (RT-qPCR) was performed on a LightCycler 96 system (Roche, Basel, Switzerland) with the FastStart Essential DNA Green Master (Roche) containing SYBR green as previously described (Ebbers et al. 2015). The following primers from Maze et al. (2010) were used: D-glyceraldehyde-3-phosphate dehydrogenase (GAPDH) forward (5′-AGGTCGGTGTGAACGGATTTG-3′), GAPDH reverse (5′-TGTAGACCATGTAGTTGAGGTCA-3′), EHMT1 forward (5′-ATTGACGCTCGGTTCTATGG-3′), EHMT1 reverse (5′-ACACTTGGAAGACCCACACC-3′), EHMT2 forward (5′-TGCCTATGTGGTCAGCTCAG-3′) and EHMT2 reverse (5′-GGTTCTTGCAGCTTCTCCAG-3′). Each sample

Table 1 Overview of mouse lines and number of animals used

Mouse strain	Immunohistochemistry						Reverse transcription quantitative polymerase chain reaction		
	P0	*P8*	*P12*	*P16*	*P25*	*1 Y*	*P0*	*P12*	*P25*
Wild-type	3	3	3	3	3	3	2	2	2
Cldn14$^{-/-}$	3	3	3	3	3	–	–	–	–
Cav1.3$^{-/-}$	3	3	3	3	3	–	–	–	–
tdTomato ^{Ptf1a}	–	–	–	–	3	–	–	–	–
tdTomato ^{Atoh7}	–	–	–	–	3	–	–	–	–

was analyzed twice with three technical and two biological replicates per run under the following thermocycling conditions: 95 °C for 5 min; 95 °C for 10 s 60 °C for 10 s, and 72 °C for 10 s for a total of 45 cycles. Additionally, melting curves were generated to verify the specificity of the products. Samples were analyzed by using the method of Pfaffl (2001) with normalization to GAPDH. Statistical analysis was performed by using the two-tailed Student's *t*-test after testing for the Gaussian distribution of the datasets with SPSS Version 23.0 (IBM, Armonk, N.Y., USA). Error bars illustrate the standard error of the mean (SEM).

Results

The expression of *Ehmt2* and its catalyzed histone 3 lysine 9 (H3K9) methylations was investigated during the postnatal development of the central auditory system in mice. We first obtained data on EHMT2 immunoreactivity during the development of the auditory system in wild-type mice and two different mouse models with hearing loss. We initially focused on major nuclei of the mouse auditory brainstem, namely the cochlear nucleus complex (CNC), the superior olivary complex (SOC) and the inferior colliculus (IC). We later included the auditory cortex (AC) in the analysis. We then carried out a developmental analysis of H3K9me1 and H3K9me2 marks in the auditory brainstem and AC of wild-type and $tdTomato^{Ptf1a}$ and $tdTomato^{Atoh7}$ mice. Finally, we considered other H3K9 methylation enzymes, namely EHMT1 and RIZ1.

EHMT2 is downregulated during maturation of auditory brainstem

To analyze the immunoreactivity against EHMT2 (EHMT2-ir) during maturation of the auditory brainstem, we investigated brain sections at P0, P8, P16, and P25. P0 and P8 represent stages prior to the onset of hearing, as the auditory system of the mouse is not fully developed at birth: the ear canals are closed, the middle ears are blocked with embryonic tissue and the hair cells of the cochlea are small and underdeveloped. The ear canal is only fully opened by approximately P10, when the Preyer reflex can be demonstrated for the first time as proof of successful sound processing (Mikaelian and Ruben 1965). P16 and P25 represent two stages after hearing onset with the latter representing the fully developed auditory system. Previous transcriptome studies had revealed that extensive changes in the genetic program of the auditory brainstem until occur the onset of hearing and only minor changes thereafter (Ehmann et al. 2013; Harris et al. 2005).

In the hindbrain of P0 mice, EHMT2 was highly abundant in all three regions of the CNC, i.e., the dorsal cochlear nucleus (DCN) and the posterior and anterior ventral cochlear nucleus (pVCN and aVCN, respectively; Fig. 2a, b). An overlay with the nuclear DAPI stain revealed the nuclear localization of the signal (Fig. 2a', a'', b'). In some intermingled cells, only the blue DAPI signal was detected, showing that EHMT2 was not present in every cell. In addition, the entire granular cell layer showed no immunoreactivity (Fig. 2b' arrowhead). The SOC of P0 mice was labeled in a similar manner, as illustrated for the lateral superior olive (LSO) and the medial nucleus of the trapezoid body (MNTB), two major nuclei of the mouse SOC (Fig. 2c). The immunoreactivity pattern at P8 was indistinguishable from that at P0. EHMT2-ir was detected in all subdivisions of the CNC and in the SOC (Fig. 2e–g). Again, immunoreactivity was restricted to the cell nuclei. Similar to the situation at P0, some cells showed no EHMT2 labeling (Fig. 2e', e'', f', g', g'').

In contrast to the situation prior to the onset of hearing, a strong decrease in signal intensity was noticed at P16. In all investigated auditory hindbrain nuclei, the signal had almost vanished and no nuclear localization was observed (Fig. 3a–d). Signal intensity was even lower at P25, when virtually no EHMT2 was detectable in the CNC or in the SOC (Fig. 3f–i).

The IC is situated in the midbrain and represents the most caudal auditory nucleus in the brainstem. This center presented an expression pattern of EHMT2 similar to that of the hindbrain nuclei. High EHMT2-ir was observed prior to the onset of hearing, whereas strong down-regulation was observed thereafter (Figs. 2d,d', h, h', 3e, e', j, j'). The observed down-regulation was consistently present in all animals investigated with little inter-individual variability as shown in Fig. 4. Developmental RT-qPCR analysis confirmed postnatal down-regulation. The reduction of *Ehmt2* expression in the brainstem between P0 and P12 was significant (mean ratio P0: 0.231 ± 0.016; P12: 0.059 ± 0.008, $P = 0.001$) and the level stayed low at P25 (mean ratio P25: 0.052 ± 0.007, $P = 0.000092$; Fig. 5a).

EHMT2 is not down-regulated in AC

During our analysis of older animals, we noticed that EHMT2-ir was still present in areas outside the brainstem. We therefore included the AC in our analysis. At all stages investigated, EHMT2-ir was present in the AC and was clearly located in cell nuclei (data not shown). To analyze whether this high expression at P25 was attributable to a delayed maturation of the AC compared with the brainstem, we extended our analyses to 1-year-old animals. Even at this age, the signal was still abundant in the AC, whereas the CNC, SOC and IC showed no immunoreactivity against the enzyme, similar to the results obtained at P16 and P25 (Fig. 6). These data identify a striking difference of EHMT2 regulation between brainstem and cortex. Whereas EHMT2 levels decline during the maturation of auditory brainstem structures, they remain high in the AC, at least throughout the first year of life.

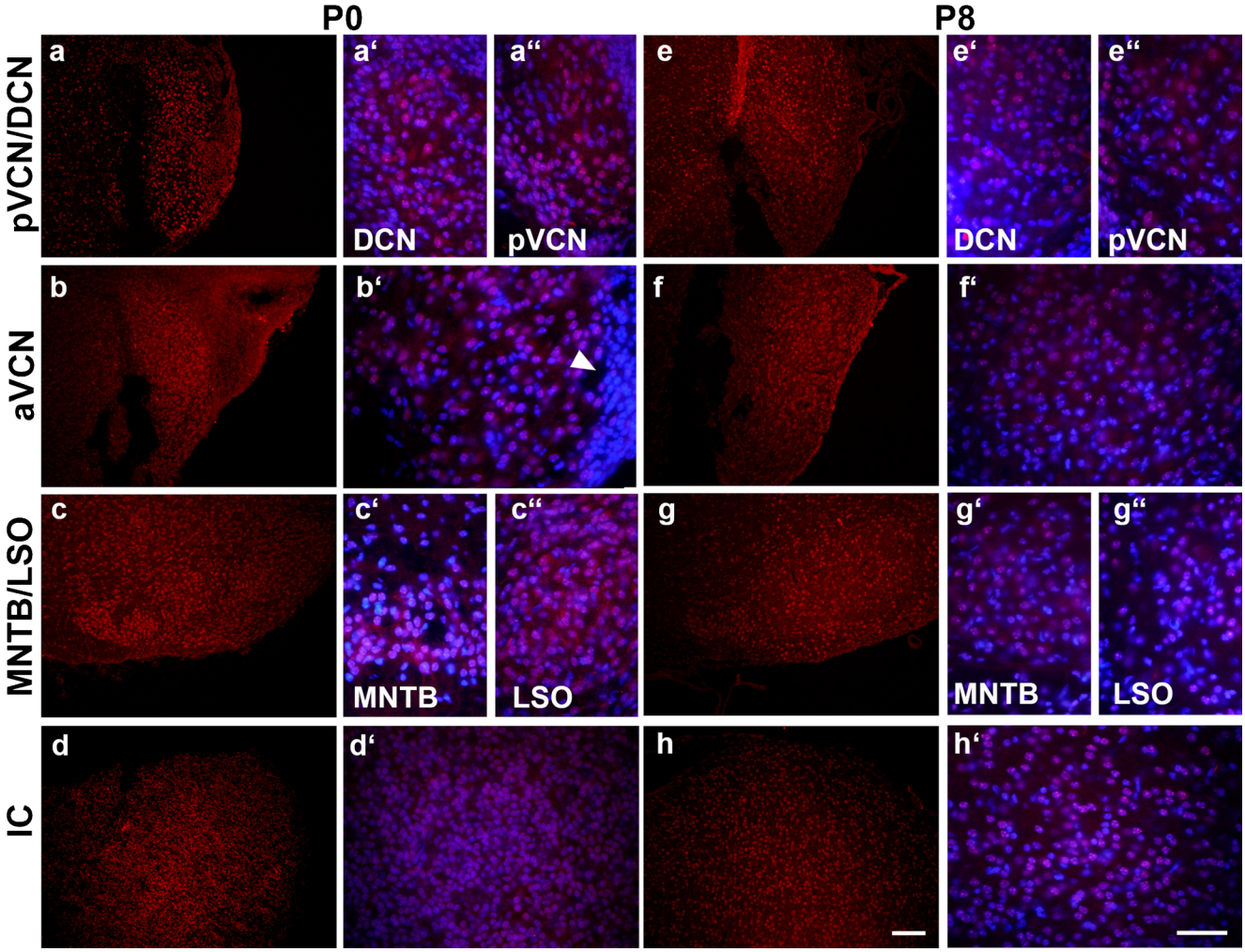

Fig. 2 EHMT2 is strongly present in auditory brainstem structures during the first postnatal week. Intense EHMT2 immunoreactivity (EHMT2-ir) is observed in all auditory brainstem structures both at postnatal day 0 (P0) and P8. Higher magnification demonstrates the respective structure overlaid with DAPI, revealing the nuclear localization of EHMT2-ir (*white arrowhead* granular cells in cochlear nucleus complex, *red* EHMT2, *blue* DAPI, *aVCN* anteroventral cochlear nucleus, *DCN* dorsal cochlear nucleus, *IC* inferior colliculus, *LSO* lateral superior olive, *MNTB* medial nucleus of the trapezoid body, *pVCN* posteroventral cochlear nucleus). Abbreviations also apply to subsequent figures. *Dorsal* is *up*, *lateral* to the *right*. *Bars* 100 μm (**a–h**), 50 μm (**a'–d'**, **a"**, **c"**, **e'–h'**, **e"**, **g"**)

To investigate whether this difference was specific to the auditory system, we also analyzed other brain areas in the brainstem and cortex at P25. Similar to the auditory system, EHMT2 expression was low in brainstem structures including the nuclei of the fifth and seventh nerve (Fig. 7a, b), whereas it stayed high in cortical areas such as the somatosensory cortex and the visual cortex (Fig. 7c, d). Thus, the developmental down-regulation of EHMT2 in the brainstem between P0 and P12 and the persistent expression of the enzyme in the cortical areas are general features. Again, quantitative RT-PCR confirmed this finding. No significant reduction in the *Ehmt2* expression level was observed in neocortical tissue between P0 and P12 or P25 (mean ratio P0: 0.223 ± 0.045; P12: 0.242 ± 0.027, $P = 0.75$; P25: 0.271 ± 0.016, $P = 0.255$; Fig. 5b).

Down-regulation of EHMT2 is independent of hearing

EHMT2 levels are regulated by external factors (Covington et al. 2011; Maze et al. 2010; Sun et al. 2012) and changes therein are thought to be critical for the interplay between the genetic and environmental determination of the phenotype (Kramer 2016). In the brainstem, we observed a strong decline of EHMT2 protein level around hearing onset. To test whether sound-driven activity had an impact on its expression, we characterized EHMT2-ir in *Cldn14*$^{-/-}$ mice (Ben-Yosef et al. 2003). These mice lack the paracellular tight junction protein Claudin 14. This results in early postnatal hair cell degeneration and profound congenital deafness, as demonstrated by the absence of auditory brainstem responses at P15-P17 (Ben-Yosef et al. 2003). Immunohistochemical analysis

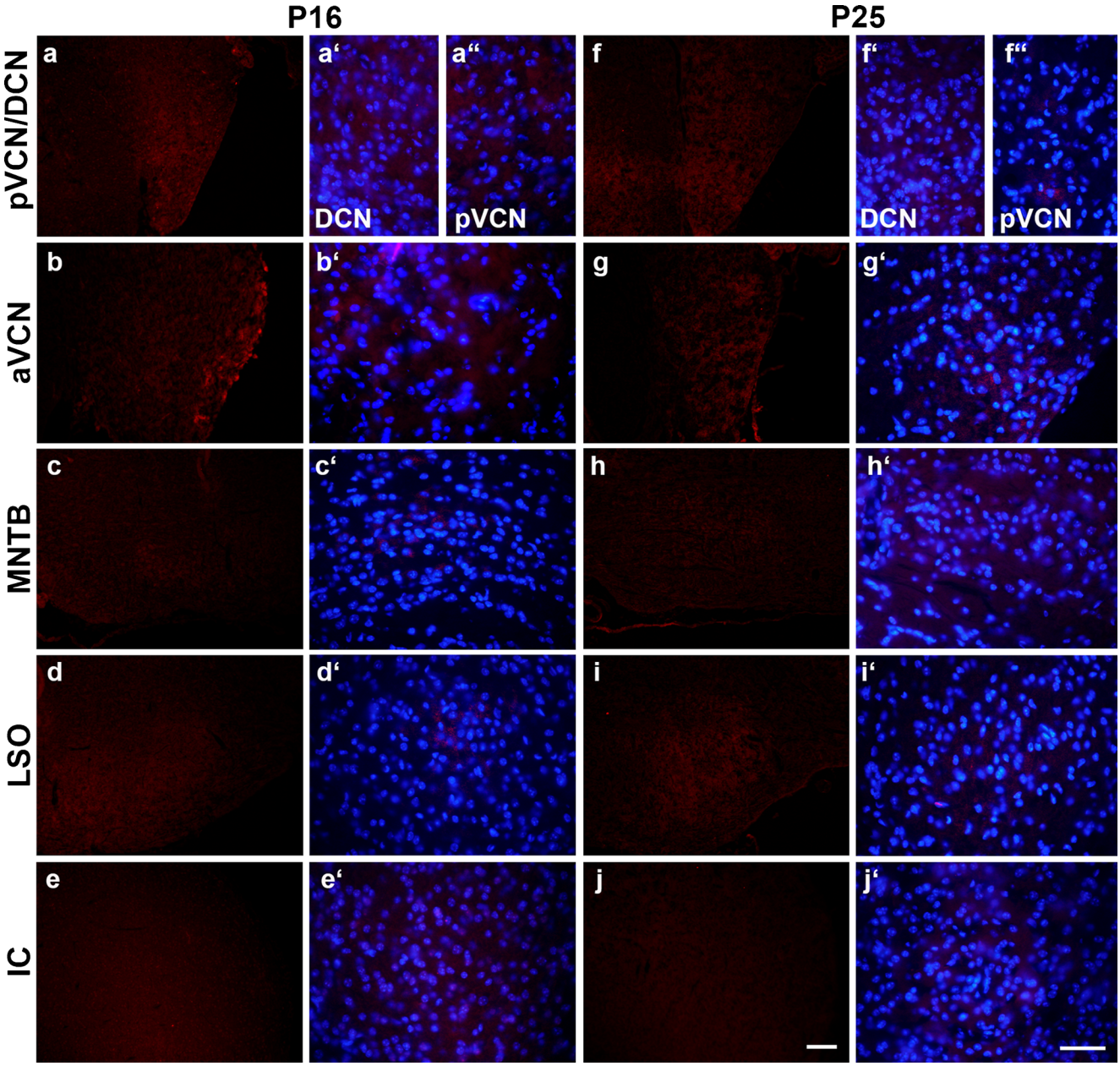

Fig. 3 Low EHMT2 immunoreactivity in auditory brainstem structures after onset of hearing. Both at P16 and P25, only weak EHMT2-ir is observed in auditory brainstem structures. Higher magnification reveals the respective structures overlaid with DAPI (*red* EHMT2, *blue* DAPI). *Dorsal* is *up*, *lateral* to the *right*. *Bars* 100 μm (**a–j**), 50 μm (**a'–e'**, **a"**, **f'–j'**, **f"**)

revealed no differences in the labeling intensity compared with the wild-type mice throughout development (data not shown). As *Cldn14*$^{-/-}$ mice might still show spontaneous neuronal activity (Wang and Bergles 2015), which might suffice to drive the postnatal down-regulation of EHMT2, we also investigated *Cacna1d*$^{-/-}$ mice, which lack the L-type Ca^{2+} channel $Ca_v1.3$ (Platzer et al. 2000). This channel is essential for neurotransmission at the inner hair cell synapse and consequently, *Cacna1d*$^{-/-}$ mice show profound deafness and lack spontaneous activity (Platzer et al. 2000). Furthermore, mice lacking $Ca_v1.3$ show severe anatomical and functional abnormalities in the auditory brainstem, such as highly increased cell loss (Hirtz et al. 2011), impaired refinement (Hirtz et al. 2012) and altered processing of auditory signals (Satheesh et al. 2012). Immunohistochemical analysis in *Cacna1d*$^{-/-}$ mice revealed no differences in EHMT2-ir compared with wild-type mice (Fig. 8). At P8, EHMT2 was highly abundant in the cell nuclei of all investigated brainstem structures and in the AC (Fig. 8a–e), whereas in P16 and P25, EHMT2-ir had almost completely vanished in the brainstem and only the blue DAPI staining was visible in the cell nuclei (Fig. 8f–i, k–n). The AC of deaf *Cacna1d*$^{-/-}$ mice showed

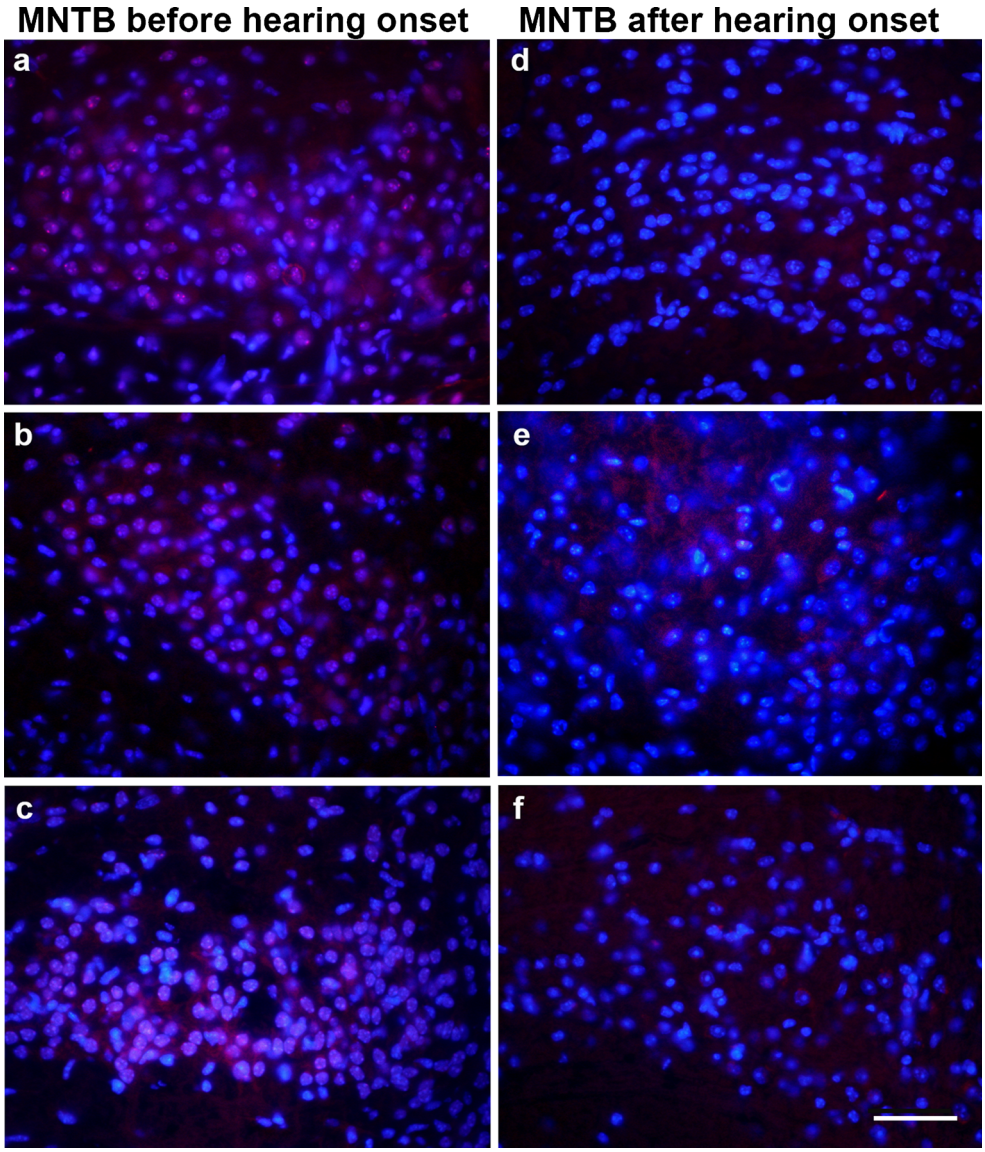

Fig. 4 Negligible inter-individual differences in labeling pattern of EHMT2 before and after onset of hearing. A consistent strong EHMT2-ir with a clear nuclear localization was seen in all animals investigated between P0 and P8 (selected examples of the MNTB from independent animals in **a–c**). No signal was detectable in animals at P16 or older (selected examples of the MNTB from independent animals in **d–f**). *Dorsal* is *up*, *lateral* to the *right*. *Bar* 50 μm

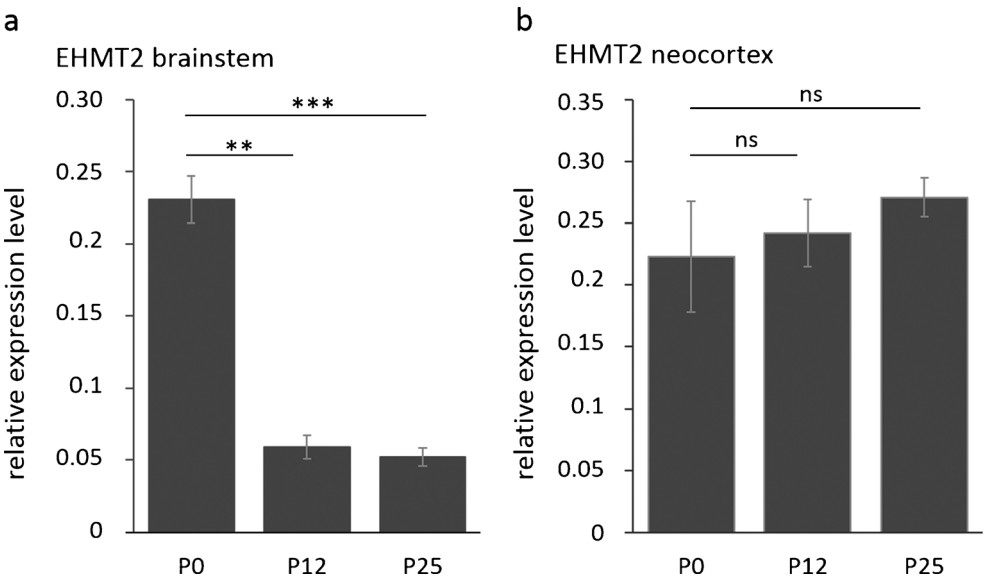

Fig. 5 Relative expression levels of *Ehmt2* in brainstem and neocortical areas. **a** Relative *Ehmt2* expression levels (± SEM) in developing mouse brainstem. A significant decrease occurred in expression at P12 and P25 compared with P0. **b** Relative *Ehmt2* expression in developing mouse neocortex. No significant up- or down-regulation of *Ehmt2* expression was observed between analyzed age groups. As a test for statistical significance, Student's *t*-test was used. $^{**}P \leq 0.05$; $^{***}P \leq 0.001$, *ns* not significant

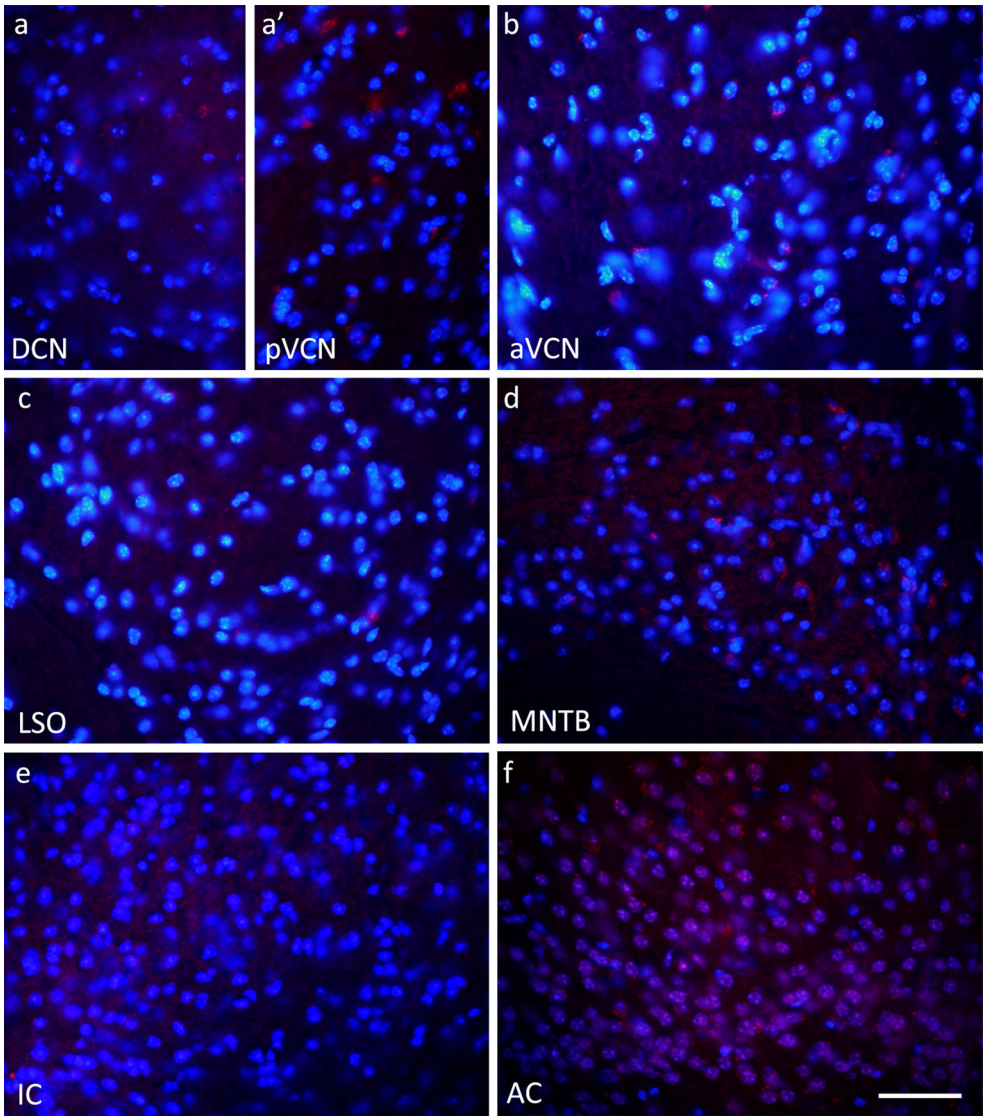

Fig. 6 Differential regulation of EHMT2 levels between auditory brainstem and auditory cortex (*AC*) in adult mice. Auditory brainstem structures show low levels of EHMT2-ir in 1-year-old mice, whereas the AC displays high EHMT2-ir. These data reveal differential regulation of this enzyme between brainstem and cortex (*red* EHMT2, *blue* DAPI). *Dorsal* is *up*, *lateral* to the *right*. *Bar* 50 μm

high EHMT2-ir at P16 and P25, thus also resembling the wild-type AC (Fig. 8j, o). These data indicate that the expression of the epigenetic modifier EHMT2 is not regulated by spontaneous or sensory driven activity in the central auditory system. This is in agreement with the observed down-regulation of EHMT2 in non-auditory brainstem structures after the first postnatal week.

Methylation persists in auditory nuclei during maturation

EHMT2 seems to be particularly important for the establishment of de novo methylations rather than for their maintenance (Leung et al. 2011). However, various data demonstrate a correlation between EHMT2 levels and H3K9 methylation under experimental conditions (Lu et al. 2013; Schaefer et al. 2009; Tachibana et al. 2002; Yu et al. 2013). The observed down-regulation of EHMT2 in the auditory brainstem provides a natural system for studying the correlation between altered EMHT2 expression and H3K9me1 and H3K9me2 levels in vivo. Furthermore, as H3K9me1 is associated with gene activation and H3K9me2 with suppression, an analysis is of interest with respect to the type of methylation that is performed by EHMT2 in the auditory system.

To address these issues, we used immunohistochemistry against either H3K9me1 (H3K9me1-ir, green) or H3K9me2 (H3K9me2-ir, red) to study their cellular pattern during the development of the auditory system. Both antibodies labeled auditory hindbrain structures at all stages analyzed, i.e., P8, P16, P25 and 1 year (Fig. 9). Of note, the labeling clearly persisted after the onset of hearing and the immunoreactivity levels appeared similar to those present in the age-matched AC (Fig. 9q–t). Thus, both types of methylation persist from P16 onwards in the brainstem, even in the absence of EHMT2, the dominant enzyme for these modifications. This is in contradiction to previous reports in which H3K9me1 and H3K9me2 were shown to be considerably decreased after

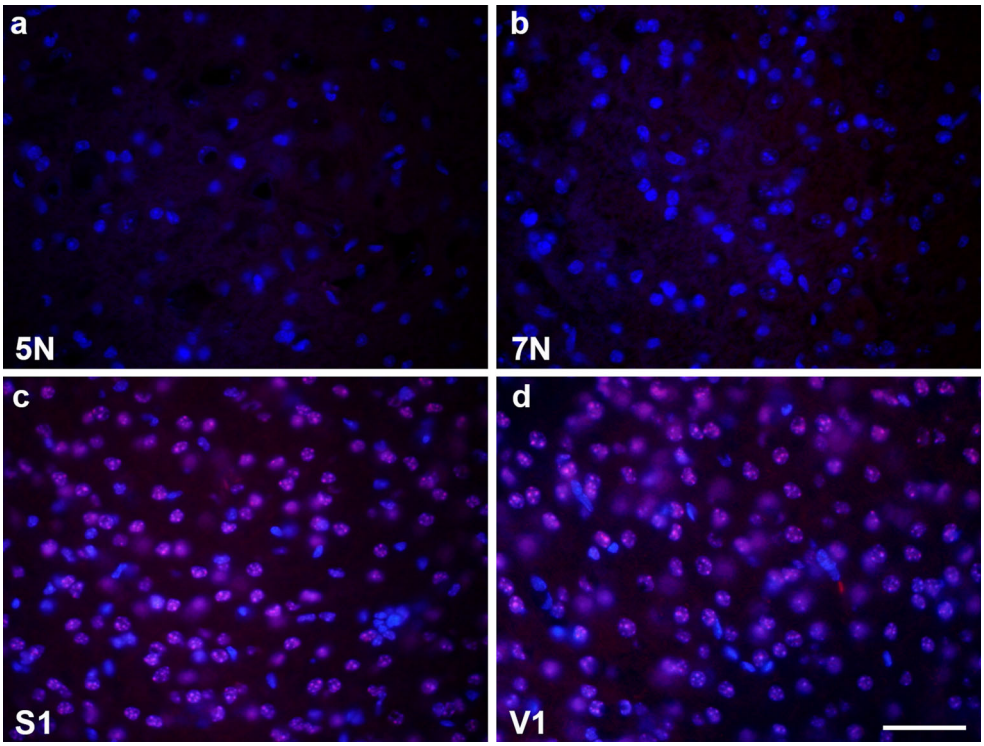

Fig. 7 Differential regulation of EHMT2 between various brain areas is a general feature in adult mice. Analysis of whole brainstem at P25 revealed no considerable EHMT2-ir. As an example, the nuclei of the fifth and seventh nerve (**a**, **b**) are shown. The whole cortex, however, was extensively labeled for EHMT2. The primary somatosensory region and the primary visual cortex (**c**, **d**) are depicted (*red* EHMT2, *blue* DAPI, *5N* trigeminal motor nucleus, *7N* facial nucleus, *S1* primary somatosensory cortex, *V1* primary visual cortex). *Dorsal* is *up*, *lateral* to the *right*. *Bar* 50 μm

the reduction of EHMT2 function by gene knockout or pharmacological intervention (Lu et al. 2013; Maze et al. 2010; Schaefer et al. 2009; Tachibana et al. 2005; Yu et al. 2013).

However, we observed developmental differences in the cellular labeling patterns of H3K9me1 or H3K9me2. At P8, most of the cells in the auditory system displayed a uniform yellowish appearance, indicating roughly the same share of mono- and dimethylations at this age (Fig. 9a, e, i, m). During maturation of the auditory system, single cells appeared more red or green in the overlay of both labels, hence indicating either more mono- or dimethylations at H3K9 (note, for instance, the red and green cells in the pVCN and MNTB at 1 year in (Fig. 9d', l). A similar change in the labeling pattern was observed during the development of the AC (Fig. 9q–t). These data suggest that individual auditory neurons adopt distinct epigenomic configurations in adulthood.

To investigate this phenomenon further and possibly to assign these different configurations to cell types, we used the *Ptf1a::Cre* and *Atoh7::Cre* driver mouse lines, both crossed to a tdTomato reporter mouse to label distinct cell populations in the auditory brainstem. Inhibitory neurons in the CNC are derived from the pancreas-specific transcription factor 1a (Ptf1a^{+}) cell lineage (Fujiyama et al. 2009) and excitatory neurons in the aVCN, which project to the SOC, express the transcription factor atonal homolog 7 (Atoh7) during development (Saul et al. 2008). In *tdTomato*^{Ptf1a} mice, we observed, in the aVCN, clear colocalization of the dtTomato signal with both predominantly monomethylated (green, arrowhead in Fig. 10a, c) and dimethylated (red, arrow in Fig. 10a, c) cells. The absence of PTFa1^{+}-derived cells in the SOC prevented a similar analysis in this center (data not shown). In *tdTomato*^{Atoh7} mice, the marked neurons of the aVCN colocalized with either predominantly monomethylated cells (green, arrowhead in Fig. 10d, f) or with cells containing both mono- and dimethylation (yellow, arrows in Fig. 10d, f). We did not observe colocalization of Atoh7^{+} neurons with predominantly dimethylated cells. Together, these data reveal the poor correlation between specific methylation patterns and cell types in the auditory hindbrain.

Immunoreactivity of other H3K9 methylation enzymes during maturation of auditory brainstem

Our analysis shows a clear down-regulation of EHMT2 in the auditory brainstem at P16 and P25 but persisting methylation of its target H3K9. This could be attributable to the expression of an additional methylase in the mature brainstem. We therefore extended our analysis to other H3K9 mono- and dimethylating enzymes. EHMT1 has been reported to form functional complexes with its close paralog EHMT2 to cooperatively methylate H3K9 (Tachibana et al. 2005). Comparable with EHMT2, EHMT1 was highly present in the nuclei of brainstem neurons at P0 (Fig. 11a–d). However, at P8, EHMT1-ir was also found in the cell somata of some auditory nuclei (Fig. 11e–h). Although a clear nuclear localization was seen in the LSO (Fig. 11h), EHMT1-ir in the MNTB was exclusively found in the soma (Fig. 11g). The

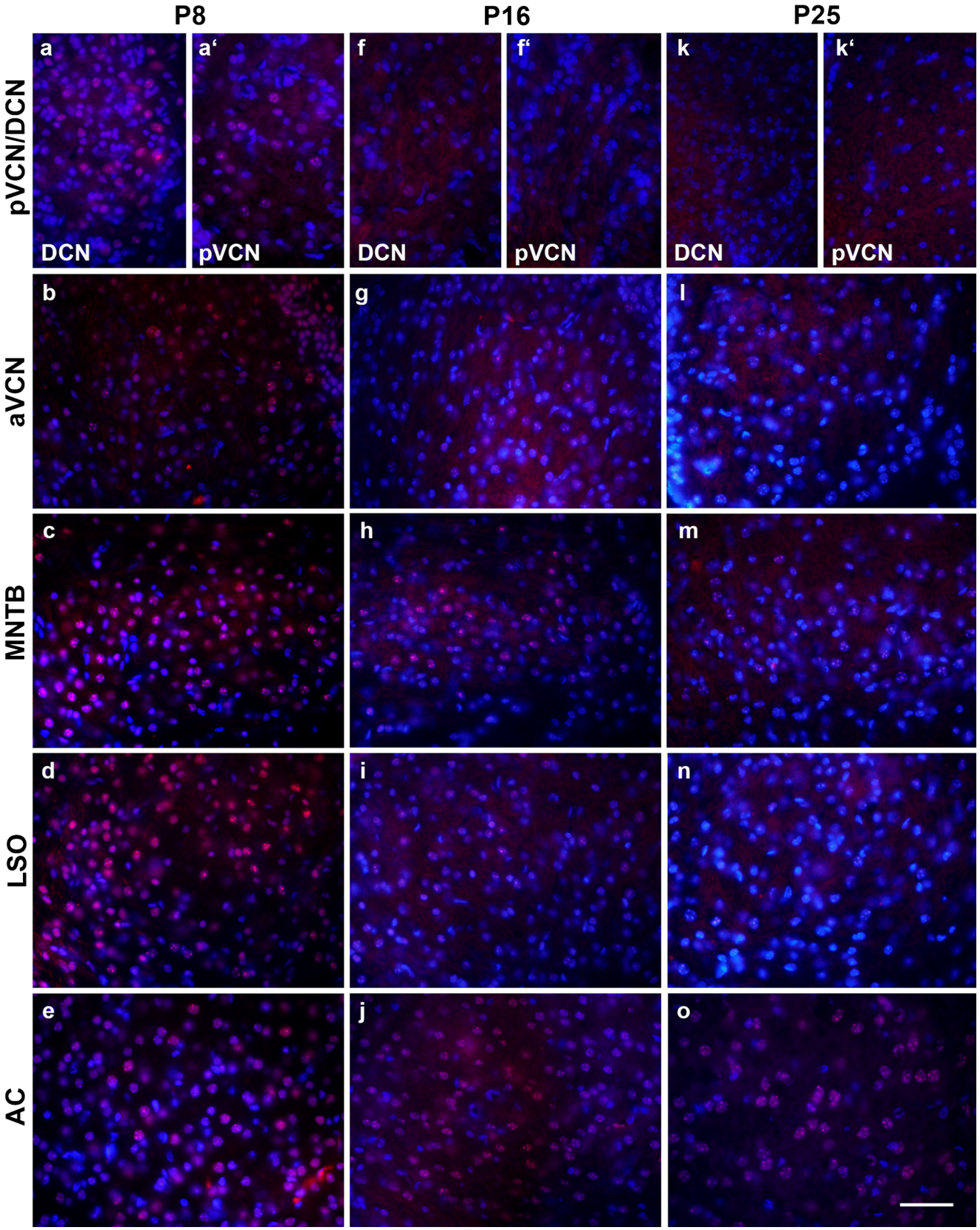

CNC showed a mixed distribution (Fig. 11e, f). At P16 and P25, EHMT1-ir resembled that of EHMT2, as no signal was detectable in the nuclei of the auditory brainstem (Fig. 11i–p). The protein was not detected in the granular cells of the CNC

◀ **Fig. 8** EHMT2 levels are independent of hearing. Analysis of EHMT2-ir in deaf *Cacna1d*$^{-/-}$ mice revealed no difference in labeling prior to and after hearing onset compared with wild-type animals. EHMT2 levels are high at P8 (**a**–**d**) and drop considerably by P16 (**f**–**i**) until labeling vanishes by P25 (**k**–**n**) in the brainstem of *Cacna1d*$^{-/-}$ mice. In contrast, levels were high at all three stages (**e**, **j**, **o**) in the AC (*red* EHMT2, *blue* DAPI). *Dorsal* is *up*, *lateral* to the *right*. *Bar* 50 μm

throughout development, again similar to EHMT2 (data not shown). At the level of the AC, distinct nuclear labeling was present at P8 (Fig. 11q), whereas at P16 and P25, no EHMT1-ir was present, which is in stark contrast to EHMT2 (Fig. 11r, s). Differential expression of *Ehmt1* in the AC was confirmed by RT-qPCR. Both in the brainstem and the neocortex, expression was high at P0 and significantly decreased at P12 and P25 (mean ratio brainstem P0: 0.132 ± 0.029; P12: 0.018 ± 0.003, $P = 0.006$; P25: 0.010 ± 0.001, $P = 0.004$; cortex P0: 0.235 ± 0.010; P12: 0.034 ± 0.004, $P = 0.000001$; P25: 0.019 ± 0.001, $P = 0.0000006$; Fig. 12). Thus, a different regulation

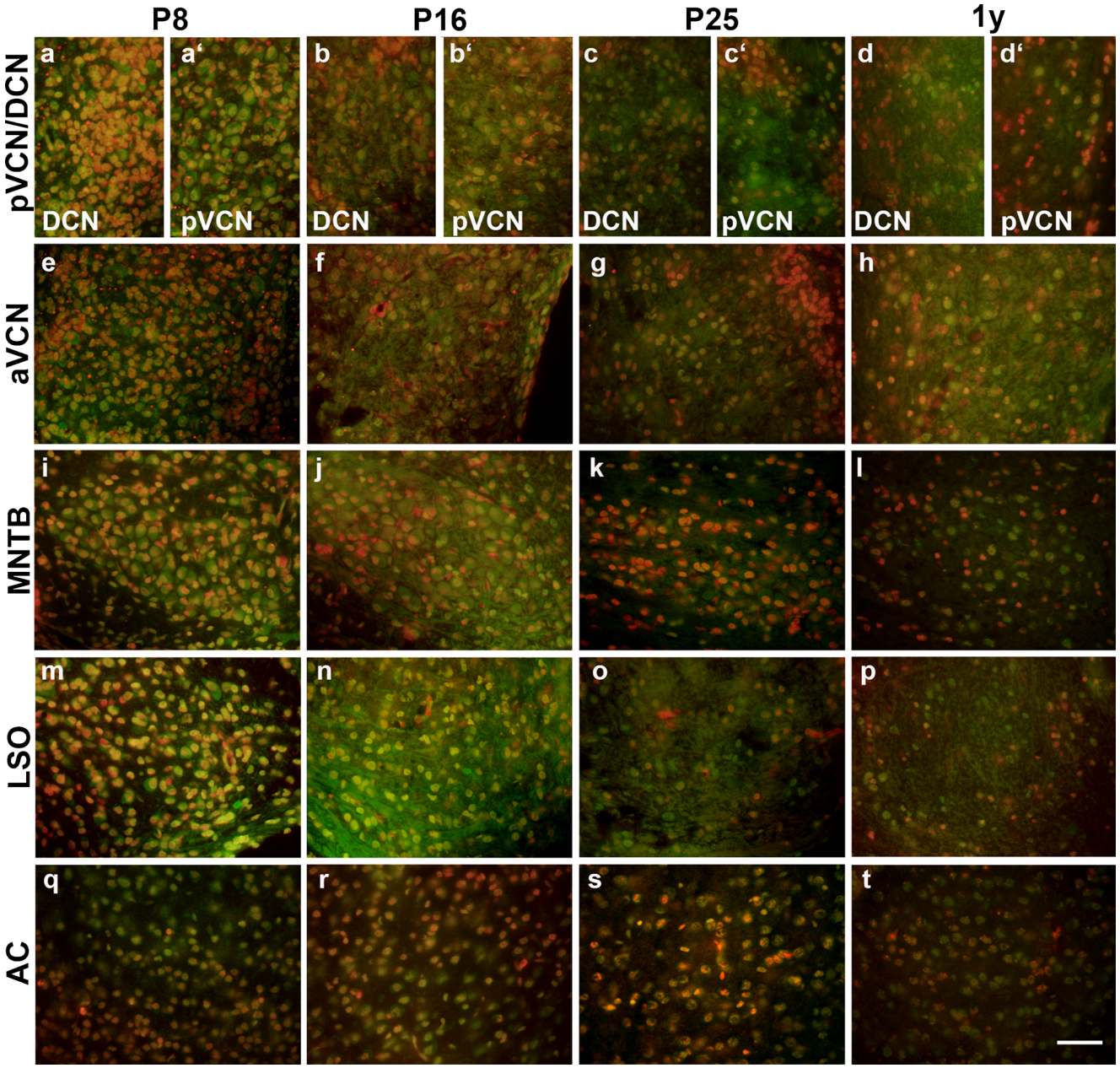

Fig. 9 Methylation on histone 3 lysine 9 persists independently of EHMT2. Monomethylations (H3K9me1) and dimethylations (H3K9me2) were highly abundant in the nuclei of the auditory brainstem and in the AC at all age stages investigated. However, a developmental switch occurred in the labeling pattern. Whereas most cells showed roughly the same share of H3K9me1 and H3K9me2 at P8 and P16, more cells were found with predominant labeling for either H3K9me1 or H3K9me2 at P25 and 1 year. No substantial difference between the various brain areas was observed (*green* H3K9me1, *red* H3K9me2). *Dorsal* is *up*, *lateral* to the *right*. *Bar* 50 μm

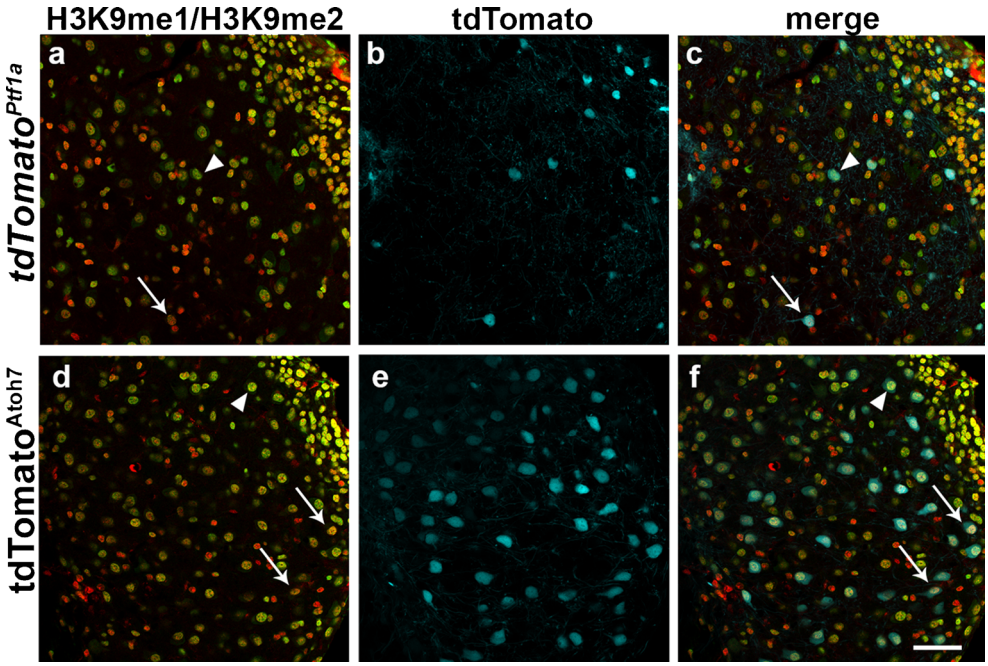

Fig. 10 No clear cell-type-specific methylation patterns in excitatory and inhibitory neurons of the aVCN. tdTomato labeled inhibitory Ptf1a$^+$ cells colocalized with both predominantly monomethylated neurons (*green*, *arrowhead* in **a**, **c**) and predominantly dimethylated neurons (*red*, *arrow* in **a**, **c**). For excitatory Atoh7$^+$ neurons, the tdTomato signal frequently colocalized with predominantly monomethylated cells (*green*, *arrowhead* in **d**, **f**) or cells with roughly the same amount of H3K9me1 and H3K9me2 (*yellow* to *orange*, *arrows* in **d**, **f**). Atoh7$^+$ cells were never predominantly dimethylated (*green* H3K9me1, *red* H3K9me2, *cyan* tdTomato). *Dorsal* is *up*, *lateral* to the *right*. *Bar* 50 μm

of these closely related enzymes occurs at the level of the neocortex.

Next, we analyzed the H3K9 methyltransferase RIZ1, which was recently identified preferentially to monomethylate H3K9 (Congdon et al. 2014). At P0, RIZ-ir was similar to that for EHMT1 and EHMT2 at the level of the auditory brainstem, with a clear nuclear localization (Fig. 13a–d). At P8, labeling remarkably resembled that of EHMT1 with a nuclear localization in the LSO (Fig. 13h), a labeled cytosol in the MNTB (Fig. 13g) and a mixed pattern in the CNC (Fig. 13e, f). Furthermore, RIZ1-ir was absent in the auditory brainstem at P16 and P25 (Fig. 13i–p). Similar to the other two methylation enzymes, the protein was not detectable in the granular cells of the CNC throughout development (data not shown). In the AC, we observed nuclear RIZ-ir up to P25, the oldest age analyzed for this enzyme (Fig. 13q–s). Its cortical expression at P25 thus resembles that of EHMT2-ir but not EHMT1-ir.

Taken together, the data indicate that all investigated H3K9 methylation enzymes are remarkably down-regulated in the mature brainstem. In contrast, their expression pattern in cortical areas varies. EHMT2 and RIZ1 are highly expressed beyond the first two weeks of life, whereas EHMT1 shows a significant down-regulation between P0 and P12, similar to its expression pattern in the brainstem.

Discussion

In this study, we report the following key observations concerning epigenetic mechanisms in the auditory system. We observed a strong down-regulation of the major H3K9 methylation enzymes EHMT1, EHMT2 and RIZ1 during the maturation of the auditory brainstem. This decrease contrasts the persistent immunoreactivity of EHMT2 and RIZ1 in the AC and the continued presence of the catalyzed H3K9me1 and H3K9me2 marks in the auditory brainstem. However, EHMT1 is also down-regulated in the adult AC. These immunohistological findings have been confirmed by RT-qPCR. Our data have importance beyond the auditory system, as they also hold true for other brain areas outside this sensory system.

Developmental down-regulation of histone 3 methylating enzymes

EHMT1, EHMT2 and RIZ1 levels decrease in the auditory brainstem of mice between P0 and P12 (Figs. 2, 3, 5, 11, 12, 13). Conditional ablation of *Ehmt1* and *Ehmt2* in the forebrain has previously been shown to entail the de-represssion of non-neuronal genes and neuronal progenitor genes that are usually present during embryonic development (Schaefer et al. 2009). Additionally, the knockdown of *Ehmt1* or *Ehmt2* in embryonic stem cells results in severe differentiation defects (Tachibana et al. 2002, 2005) and *Ehmt2* deficiency leads to the expression of neuronal genes in cell lines of non-neuronal origin (Ding et al. 2008; Roopra et al. 2004). These data have led to the conclusion that these enzymes are important for the maintenance of cell identity. However, this contrasts our finding in the auditory brainstem. Here, the disappearance of EHMT1 and EHMT2 occurs as a natural process at a time when these neurons acquire their cellular and genetic identity (Nothwang et al. 2015). The auditory neurons instead appear to down-regulate these methyltransferases in order to fix their

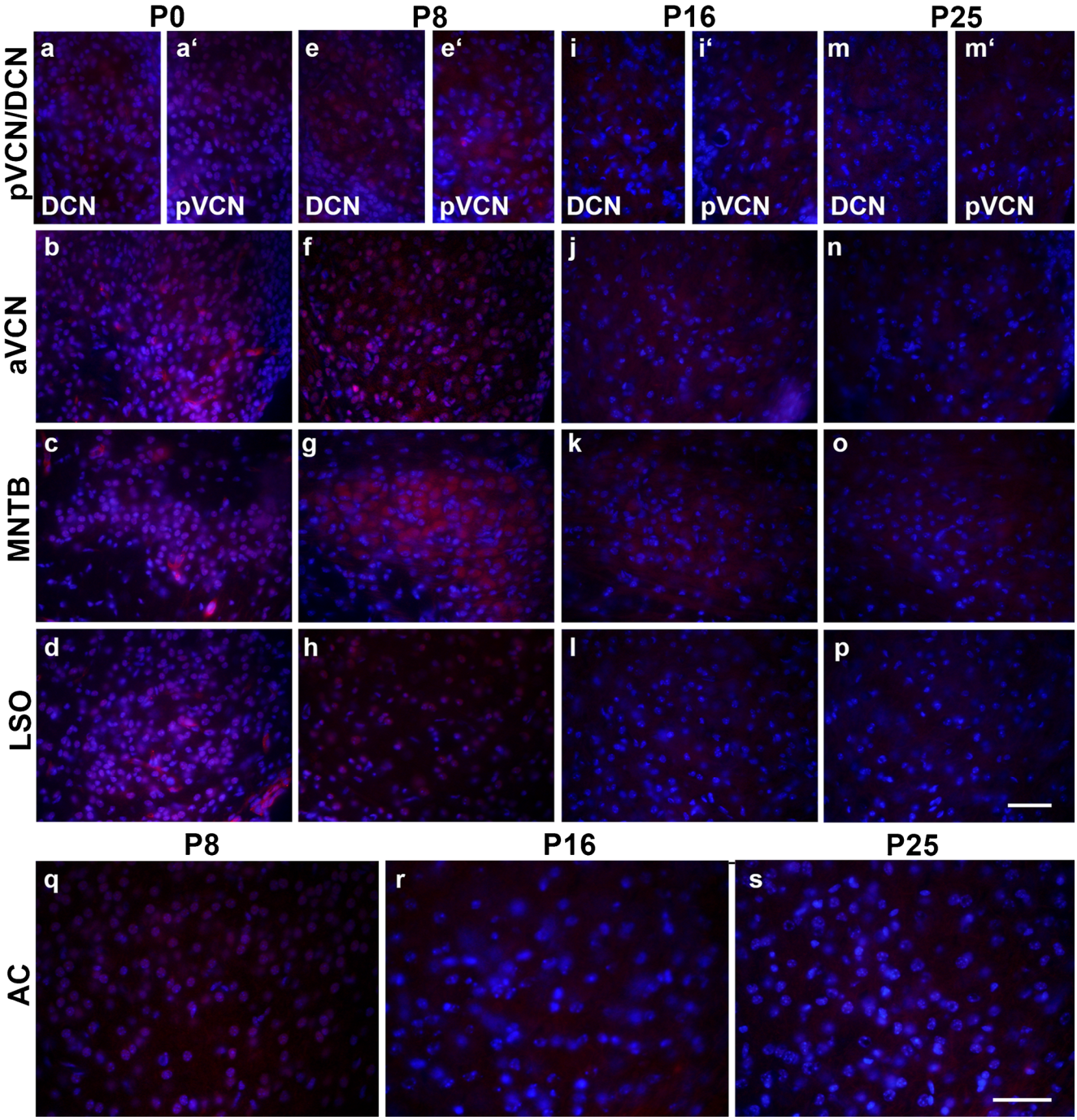

Fig. 11 Immunoreactivity of EHMT1 in the auditory brainstem and AC before and after the onset of hearing. Consistent with EHMT2-ir, EHMT1 was highly present in the nuclei of the auditory brainstem at P0 (**a**–**d**). At P8, a redistribution of the signal occurred from the nucleus to the cytoplasm in the MNTB (**g**) and partially in the CNC (**e**, **f**), whereas nuclear labeling persisted in the LSO (**h**). At P16 and P25, no EHMT1-ir was detectable at the level of the brainstem (**i**–**p**). Nuclear labeling of EHMT1 in the AC was observed (**q**) at P8 but the signal was absent (**r**, **s**) at P16 and P25 (*red* EHMT1, *blue* DAPI). *Dorsal* is *up*, *lateral* to the *right*. *Bars* 50 μm

genetic programs and seem to have a low demand for genomic reprograming in the mature state. This is in agreement with the observations of only minor changes in gene expression after P16 in the SOC (Ehmann et al. 2013) and of the very low degree of synaptic plasticity of auditory brainstem circuits compared with non-auditory structures (Friauf et al. 2015). The broad down-regulation of H3K9 methyltransferases in the brainstem is compatible with this concept, as this part of the brain is essential for basic functions of the organisms such as breathing. These processes rely on hardwired circuits with a rather stereotypic output and a low degree of plasticity in response to external factors. This contrasts the requirements

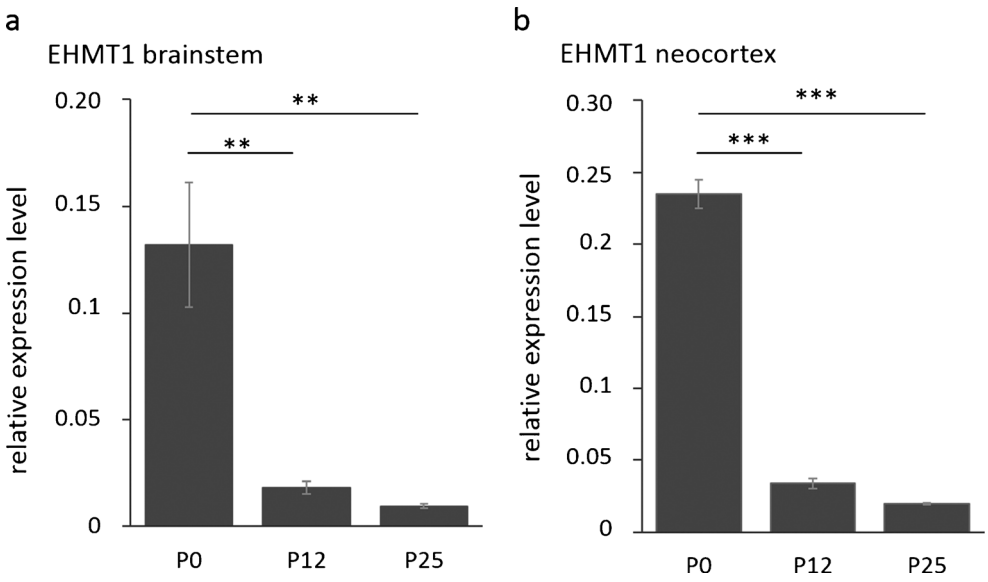

Fig. 12 Relative expression levels of *Ehmt1* in the brainstem and neocortical areas. **a** Relative *Ehmt1* expression levels (± SEM) in the brainstem of mice during postnatal development. A significant decrease occurs in expression between P0 compared with P12 and P25. **b** Relative *Ehmt1* expression in the neocortex of mice during postnatal development. *Ehmt1* levels were significantly decreased in the neocortex at P12 and P25 compared with P0. As a test for statistical significance, Student's *t*-test was used. $^{**}P \leq 0.05$; $^{***}P \leq 0.001$

in cortical structures in which epigenetic marks are important for adult plasticity and adaptations to external signals (Gupta-Agarwal et al. 2012; Kramer 2016; Maze et al. 2010; Schaefer et al. 2009). Surprisingly, we found a highly significant reduction of EHMT1 in the neocortex of adult mice, whereas EHMT2 and RIZ1 still show high expression levels and immunoreactivity in cortical areas.

In addition to the down-regulation of EHMT1 and RIZ1 in the brainstem, we demonstrated a cellular redistribution of these enzymes from the nucleus to the cytoplasm at P8 in the MNTB and partially in the CNC (Figs. 11g, 13g). This altered localization of EHMT1 and RIZ1 suggests a switch in substrate preference at that age. However, no non-histone substrate is known for RIZ1 (Zhang et al. 2012) and only one non-histone substrate has been determined for EHMT1, namely the partially cytoplasmically located p53 protein (Chen et al. 2010; Zhang et al. 2012).

Persistent methylation of H3K9

Methylations at lysine residues were believed to be very stable (Byvoet et al. 1972). Nevertheless, the knockdown or ablation of *Ehmt1* or *Ehmt2* are usually paralleled by a reduction of H3K9me1 and H3K9me2 (Lu et al. 2013; Schaefer et al. 2009; Tachibana et al. 2002; Yu et al. 2013). Furthermore, during the development of the zebrafish retina, both EHMT2 expression and H3K9me2 marks vanish in parallel (Rao et al. 2010). The persistance of the mono- and dimethylations in the auditory brainstem was therefore unexpected after the down-regulation of all three enzymes investigated (Fig. 9). This indicates either that the methylation marks set by EHMT1, EHMT2, or RIZ1 actually persist for at least 1 year of life or, more likely, that the methylations are established or maintained by one of the other numerous H3K9 methyltransferases. EHMT1 and EHMT2 transfer methyl groups via their SET domain (Dillon et al. 2005). The genome encodes more than 50 SET-domain-containing proteins of which only a few have been enzymatically characterized (Tachibana et al. 2005). Hence, a multitude of enzymes might compensate for the down-regulation of EHMT1, EHMT2 and RIZ1. The presence of additional histone 3 methylases in the brainstem is supported by the observation of H3K9me1 and H3K9me2 in granular cells of the CNC, despite the absence of the three enzymes analyzed.

Methylation pattern and cell-types

The cell-specific activity of methylation enzymes other than EMHT2 might also explain the variability of the H3k9me1 and H3K9me2 levels between distinct cells in the adult organism (Fig. 9). Alternatively, the differential dominance of either H3K9me1 or H3k9me2 in individual cells might result from the different action of H3K9-specific demethylases (Shi 2007). In addition, our immunohistochemical analyses provide no spatial resolution at the genomic level and even cells with a similar labeling pattern could therefore possess quite distinct H3K9me1 and H3K9me2 marks. A recent analysis of DNA methylation revealed marked differences between different neuronal cell types (Mo et al. 2015; Sharma et al. 2016). The observed differences in the ratio between H3K9me1 and H3K9me2 might therefore be related to distinct auditory cell types. To address this issue, we analyzed the H3K9me1 and H3K9me2 patterns in two different mouse lines, with either inhibitory or excitatory neurons labeled in the aVCN. We observed no correlation between the methylation pattern and labeling of inhibitory neurons, whereas excitatory cells exclusively showed an intense reactivity for H3K9me1 or cells with roughly the same amount of

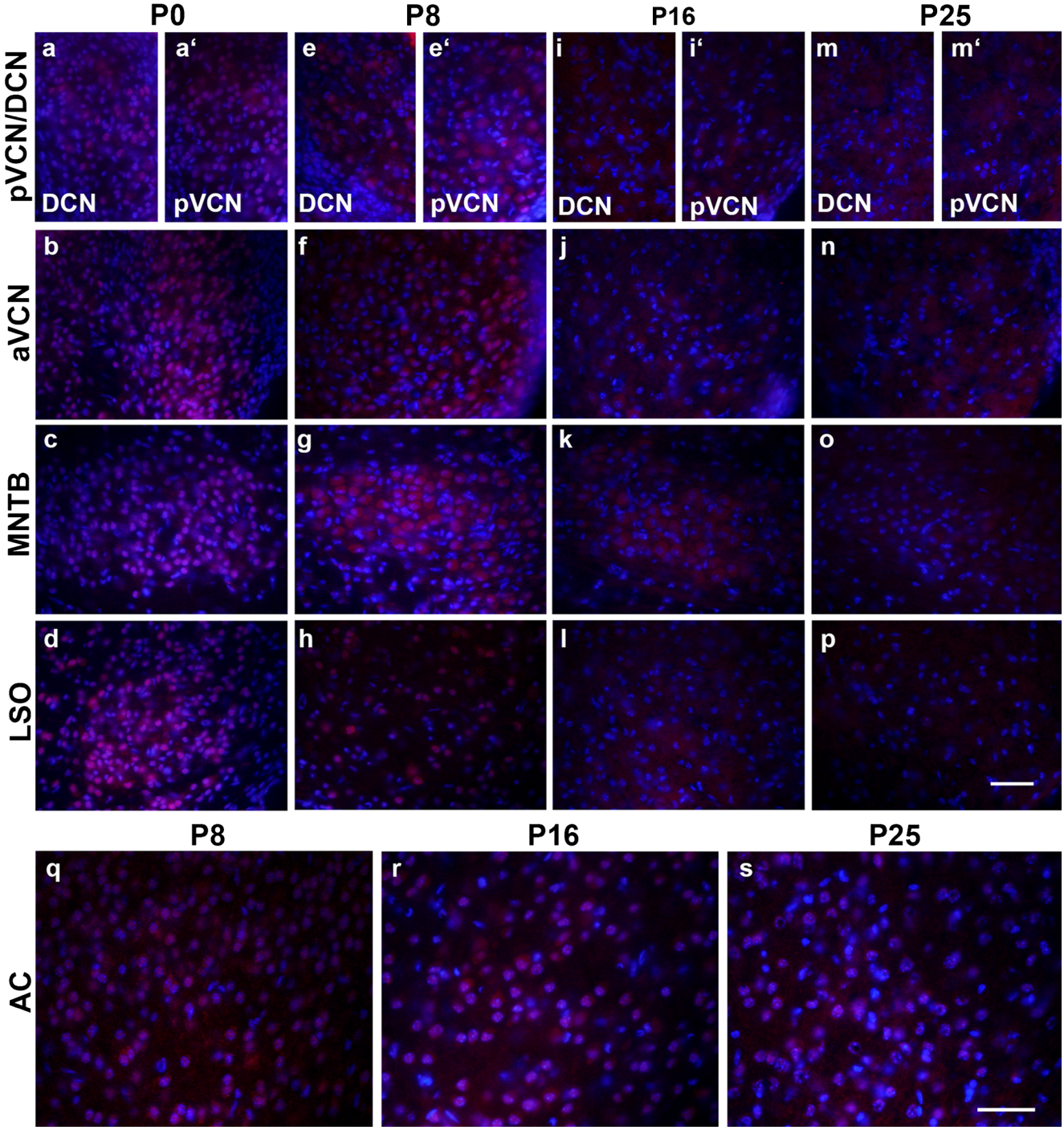

Fig. 13 Immunoreactivity of RIZ1 in the auditory brainstem and AC before and after onset of hearing. RIZ1 was highly present in the nuclei of the auditory brainstem at P0 (**a–d**), comparable with EHMT1-ir and EHMT2-ir. At P8, a redistribution of the signal took place from the nucleus to the cytoplasm in the MNTB (**g**) and partially in the CNC (**e**, **f**), whereas the LSO maintained a nuclear labeling pattern (**h**). No detectable RIZ1-ir was seen in the auditory brainstem (**i–p**) at P16 and P25. RIZ-ir with a nuclear localization was present in the AC (**q–s**) at P8, P16 and P25 (*red* RIZ1, *blue* DAPI). *Dorsal* is *up*, *lateral* to the *right*. *Bars* 50 μm

H3K9me1 and H3K9me2 (Fig. 10). This suggests a certain correlation between cell type and methylation state. However, the methylation pattern in the DCN and the MNTB argue against this assumption. The DCN is a highly organized structure with layer-specific cell types (Oertel and Young 2004) but we could not link layers or cell types such as fusiform cells to differences in H3K9me1 and H3K9me2 labeling. Furthermore, MNTB neurons represent a highly homogeneous population of principal cells and yet exhibit marked differences in the ratio of H3K9me1 and H3K9me2

(Fig. 9l). A detailed analysis of more markers for various cell types and additional methylation marks is needed to clarify the relation between cell type and methylation state.

Epigenetics in hearing impairment

A clinically highly relevant issue in hearing research is the role of epigenetic mechanisms in normal and dysfunctional hearing, as it holds the promise of pharmacology-based intervention and therapy (Layman and Zuo 2014). So far, both beneficial and harmful roles of epigenetic mechanisms have been identified. The pharmacological inhibition of EHMT2 decreases H3K9me2 in the organ of Corti in vitro and in vivo and is able to prevent hair cell loss (Yu et al. 2013). Valproic acid, a pan histone deacetylase inhibitor, has been shown to preserve hearing ability in the DBA/2 J mouse, a model of progressive hearing loss (Mutai et al. 2015). On the other hand, mutations in *EHMT1* are causative, in humans, for Kleefstra syndrome, which is associated with sensorineural hearing loss (Kleefstra et al. 2005). Here, we investigated whether hearing loss might be associated with altered EHMT2 expression. All types of congenital deafness share an altered activity pattern in the central auditory system (Nothwang et al. 2015). This might impair the proper unfolding of the genetic program, ultimately impairing auditory rehabilitation by peripheral hearing aids such as cochlear implants (Willaredt et al. 2014). Indeed, deafness has been shown to be linked to large scale alterations in gene expression in the central auditory system (Holt et al. 2005). However, both congenital deaf mouse lines tested in this study show EHMT2 expression levels indistinguishable from those of the wild-type (Fig. 8). This is also in agreement with a developmental down-regulation of the enzyme in other brainstem areas, indicating that such a change occurs independently of sensory activity. In the future, other epigenetic markers should therefore be investigated for their association with activity-dependent processes in the auditory system.

Concluding remarks

Our expression analysis is the first undertaking on the major H3K9 methyltransferases during the development of a neurosensory system. This work revealed the striking differences in the expression and labeling patterns along the auditory system and between the enzymes and their catalyzed epigenetic marks. The study of the function of these enzymes along the auditory pathway should therefore be of considerable interest. The availability of floxed *Ehmt1* and *Ehmt2* alleles (Schaefer et al. 2009) and several Cre-driver lines for conditional ablation in the auditory system will pave the way for such investigations, which hold the promise of making important contributions to the emerging field of epigenetics in the auditory system.

Acknowledgments We thank Martina Reents for expert help with genotyping and Dr. Gan and Dr. Wright for allowing use of the *Ptf1a:: Cre* and *Atoh7:: Cre* driver lines.

References

Antignano F, Burrows K, Hughes MR, Han JM, Kron KJ, Penrod NM, Oudhoff MJ, Wang SKH, Min PH, Gold MJ, Chenery AL, Braam MJS, Fung TC, Rossi FMV, McNagny KM, Arrowsmith CH, Lupien M, Levings MK, Zaph C (2014) Methyltransferase G9A regulates T cell differentiation during murine intestinal inflammation. J Clin Invest 124:1945–1955. doi:10.1172/JCI69592

Barski A, Cuddapah S, Cui K, Roh T-Y, Schones DE, Wang Z, Wei G, Chepelev I, Zhao K (2007) High-resolution profiling of histone methylations in the human genome. Cell 129:823–837. doi:10.1016/j.cell.2007.05.009

Ben-Yosef T, Belyantseva IA, Saunders TL, Hughes ED, Kawamoto K, Itallie V, Christina M, Beyer LA, Halsey K, Gardner DJ, Wilcox ER, Rasmussen J, Anderson JM, Dolan DF, Forge A, Raphael Y, Camper SA, Friedman TB (2003) Claudin 14 knockout mice, a model for autosomal recessive deafness DFNB29, are deaf due to cochlear hair cell degeneration. Hum Mol Genet 12:2049–2061

Byvoet P, Shepherd GR, Hardin JM, Noland BJ (1972) The distribution and turnover of labeled methyl groups in histone fractions of cultured mammalian cells. Arch Biochem Biophys 148:558–567

Chen L, Li Z, Zwolinska AK, Smith MA, Cross B, Koomen J, Yuan Z-M, Jenuwein T, Marine J-C, Wright KL, Chen J (2010) MDM2 recruitment of lysine methyltransferases regulates p53 transcriptional output. EMBO J 29:2538–2552. doi:10.1038/emboj.2010.140

Congdon LM, Sims JK, Tuzon CT, Rice JC (2014) The PR-Set7 binding domain of Riz1 is required for the H4K20me1-H3K9me1 trans-tail "histone code" and Riz1 tumor suppressor function. Nucleic Acids Res 42:3580–3589. doi:10.1093/nar/gkt1377

Covington HE, Maze I, Sun H, Bomze HM, DeMaio KD, Wu EY, Dietz DM, Lobo MK, Ghose S, Mouzon E, Neve RL, Tamminga CA, Nestler EJ (2011) A role for repressive histone methylation in cocaine-induced vulnerability to stress. Neuron 71:656–670. doi:10.1016/j.neuron.2011.06.007

Dillon SC, Zhang X, Trievel RC, Cheng X (2005) The SET-domain protein superfamily: protein lysine methyltransferases. Genome Biol 6:227. doi:10.1186/gb-2005-6-8-227

Ding N, Zhou H, Esteve P-O, Chin HG, Kim S, Xu X, Joseph SM, Friez MJ, Schwartz CE, Pradhan S, Boyer TG (2008) Mediator links epigenetic silencing of neuronal gene expression with x-linked mental retardation. Mol Cell 31:347–359. doi:10.1016/j.molcel.2008.05.023

Ebbers L, Satheesh SV, Janz K, Ruttiger L, Blosa M, Hofmann F, Morawski M, Griesemer D, Knipper M, Friauf E, Nothwang HG (2015) L-type calcium channel Cav1.2 is required for maintenance of auditory brainstem nuclei. J Biol Chem 290:23692–23710. doi:10.1074/jbc.M115.672675

Ehmann H, Hartwich H, Salzig C, Hartmann N, Clément-Ziza M, Ushakov K, Avraham KB, Bininda-Emonds ORP, Hartmann AK, Lang P, Friauf E, Nothwang HG (2013) Time-dependent gene expression analysis of the developing superior olivary complex. J Biol Chem 288:25865–25879. doi:10.1074/jbc.M113.490508

Friauf E (2004) Developmental changes and cellular plasticity in the superior olivary complex. In: Parks TN, Rubel EW, Fay RR, Popper AN (eds) Plasticity of the auditory system. Springer, New York, pp 49–95

Friauf E, Fischer AU, Fuhr MF (2015) Synaptic plasticity in the auditory system: a review. Cell Tissue Res 361:177–213. doi:10.1007/s00441-015-2176-x

Fujiyama T, Yamada M, Terao M, Terashima T, Hioki H, Inoue YU, Inoue T, Masuyama N, Obata K, Yanagawa Y, Kawaguchi Y, Nabeshima Y-I, Hoshino M (2009) Inhibitory and excitatory subtypes ofcochlear nucleus neurons are defined by distinct bHLH transcription factors, Ptf1a and Atoh1. Development 136:2049–2058. doi:10.1242/dev.033480

Goldberg AD, Allis CD, Bernstein E (2007) Epigenetics: a landscape takes shape. Cell 128:635–638. doi:10.1016/j.cell.2007.02.006

Gupta-Agarwal S, Franklin AV, Deramus T, Wheelock M, Davis RL, McMahon LL, Lubin FD (2012) G9a/GLP histone lysine dimethyltransferase complex activity in the hippocampus and the entorhinal cortex is required for gene activation and silencing during memory consolidation. J Neurosci 32:5440–5453. doi:10.1523/JNEUROSCI.0147-12.2012

Harris JA, Hardie NA, Bermingham-McDonogh O, Rubel EW (2005) Gene expression differences over a critical period of afferent-dependent neuron survival in the mouse auditory brainstem. J Comp Neurol 493:460–474

Harris JA, Iguchi F, Seidl AH, Lurie DI, Rubel EW (2008) Afferent deprivation elicits a transcriptional response associated with neuronal survival after a critical period in the mouse cochlear nucleus. J Neurosci 28:10990–11002

Hirtz JJ, Boesen M, Braun N, Deitmer JW, Kramer F, Lohr C, Muller B, Nothwang HG, Striessnig J, Lohrke S, Friauf E (2011) Cav1.3 calcium channels are required for normal development of the auditory brainstem. J Neurosci 31:8280–8294

Hirtz JJ, Braun N, Griesemer D, Hannes C, Janz K, Lohrke S, Muller B, Friauf E (2012) Synaptic refinement of an inhibitory topographic map in the auditory brainstem requires functional Cav1.3 calcium channels. J Neurosci 32:14602–14616

Holt AG, Asako M, Lomax CA, MacDonald JW, Tong L, Lomax MI, Altschuler RA (2005) Deafness-related plasticity in the inferior colliculus: gene expression profiling following removal of peripheral activity. J Neurochem 93:1069–1086

Kandler K, Clause A, Noh J (2009) Tonotopic reorganization of developing auditory brainstem circuits. Nat Neurosci 12:711–717

Kawaguchi Y, Cooper B, Gannon M, Ray M, Macdonald RJ, Wright CVE (2002) The role of the transcriptional regulator Ptf1a in converting intestinal to pancreatic progenitors. Nat Genet 32:128–134. doi:10.1038/ng959

Kleefstra T, Smidt M, Banning MJG, Oudakker AR, Esch H van, Brouwer APM de, Nillesen W, Sistermans EA, Hamel BCJ, Bruijn D de, Fryns J-P, Yntema HG, Brunner HG, Vries BBA de, Bokhoven H van (2005) Disruption of the gene euchromatin histone methyl transferase1 (Eu-HMTase1) is associated with the 9q34 subtelomeric deletion syndrome. J Med Genet 42:299–306. doi:10.1136/jmg.2004.028464

Kramer JM (2016) Regulation of cell differentiation and function by the euchromatin histone methyltransferases G9a and GLP. Biochem Cell Biol 94:26-32. doi:10.1139/bcb-2015-0017

Kramer JM, Kochinke K, Oortveld MAW, Marks H, Kramer D, Jong EK de, Asztalos Z, Westwood JT, Stunnenberg HG, Sokolowski MB, Keleman K, Zhou H, Bokhoven H van, Schenck A (2011) Epigenetic regulation of learning and memory by Drosophila EHMT/G9a. PLoS Biol 9:e1000569. doi:10.1371/journal.pbio.1000569

Layman WS, Zuo J (2014) Epigenetic regulation in the inner ear and its potential roles in development, protection, and regeneration. Front Cell Neurosci 8:446. doi:10.3389/fncel.2014.00446

Leung DC, Dong KB, Maksakova IA, Goyal P, Appanah R, Lee S, Tachibana M, Shinkai Y, Lehnertz B, Mager DL, Rossi F, Lorincz MC (2011) Lysine methyltransferase G9a is required for de novo DNA methylation and the establishment, but not the maintenance, of proviral silencing. Proc Natl Acad Sci U S A 108:5718–5723. doi:10.1073/pnas.1014660108

Ling BMT, Bharathy N, Chung T-K, Kok WK, Li S, Tan YH, Rao VK, Gopinadhan S, Sartorelli V, Walsh MJ, Taneja R (2012) Lysine methyltransferase G9a methylates the transcription factor MyoD and regulates skeletal muscle differentiation. Proc Natl Acad Sci U S A 109:841–846. doi:10.1073/pnas.1111628109

Lister R, Mukamel EA, Nery JR, Urich M, Puddifoot CA, Johnson ND, Lucero J, Huang Y, Dwork AJ, Schultz MD, Yu M, Tonti-Filippini J, Heyn H, Hu S, Wu JC, Rao A, Esteller M, He C, Haghighi FG, Sejnowski TJ, Behrens MM, Ecker JR (2013) Global epigenomic reconfiguration during mammalian brain development. Science 341:1237905. doi:10.1126/science.1237905

Lu Z, Tian Y, Salwen HR, Chlenski A, Godley LA, Raj JU, Yang Q (2013) Histone-lysine methyltransferase EHMT2 is involved in proliferation, apoptosis, cell invasion, and DNA methylation of human neuroblastoma cells. Anti-Cancer Drugs 24:484–493. doi:10.1097/CAD.0b013e32835ffdbb

Madisen L, Zwingman TA, Sunkin SM, Oh SW, Zariwala HA, Gu H, Ng LL, Palmiter RD, Hawrylycz MJ, Jones AR, Lein ES, Zeng H (2010) A robust and high-throughput Cre reporting and characterization system for the whole mouse brain. Nat Neurosci 13:133–140. doi:10.1038/nn.2467

Maze I, Covington HE, Dietz DM, LaPlant Q, Renthal W, Russo SJ, Mechanic M, Mouzon E, Neve RL, Haggarty SJ, Ren Y, Sampath SC, Hurd YL, Greengard P, Tarakhovsky A, Schaefer A, Nestler EJ (2010) Essential role of the histone methyltransferase G9a in cocaine-induced plasticity. Science 327:213–216. doi:10.1126/science.1179438

Mikaelian D, Ruben RJ (1965) Development of hearing in the normal Cba-J mouse: correlation of physiological observations with behavioral responses and with cochlear anatomy. Acta Otolaryngol 59:451–461. doi:10.3109/00016486509124579

Mo A, Mukamel EA, Davis FP, Luo C, Henry GL, Picard S, Urich MA, Nery JR, Sejnowski TJ, Lister R, Eddy SR, Ecker JR, Nathans J (2015) Epigenomic signatures of neuronal diversity in the mammalian brain. Neuron 86:1369–1384. doi:10.1016/j.neuron.2015.05.018

Mostafapour SP, Cochran SL, Del Puerto NM, Rubel EW (2000) Patterns of cell death in mouse anteroventral cochlear nucleus neurons after unilateral cochlea removal. J Comp Neurol 426:561–571

Mutai H, Miya F, Fujii M, Tsunoda T, Matsunaga T (2015) Attenuation of progressive hearing loss in DBA/2J mice by reagents that affect epigenetic modifications is associated with up-regulation of the zinc importer Zip4. PLoS ONE 10:e0124301. doi:10.1371/journal.pone.0124301

Nothwang HG, Ebbers L, Schluter T, Willaredt MA (2015) The emerging framework of mammalian auditory hindbrain development. Cell Tissue Res 361:33–48. doi:10.1007/s00441-014-2110-7

Oertel D, Young ED (2004) What's a cerebellar circuit doing in the auditory system? Trends Neurosci 27:104–110

Ogawa H, Ishiguro K-I, Gaubatz S, Livingston DM, Nakatani Y (2002) A complex with chromatin modifiers that occupies E2F- and Myc-responsive genes in G0 cells. Science 296:1132–1136. doi:10.1126/science.1069861

Pfaffl MW (2001) A new mathematical model for relative quantification in real-time RT-PCR. Nucleic Acids Res 29:e45

Platzer J, Engel J, Schrott-Fischer A, Stephan K, Bova S, Chen H, Zheng H, Striessnig J (2000) Congenital deafness and sinoatrial node dysfunction in mice lacking class D L-type Ca^{2+} channels. Cell 102:89–97

Rao RC, Tchedre KT, Malik MTA, Coleman N, Fang Y, Marquez VE, Chen DF (2010) Dynamic patterns of histone lysine methylation in the developing retina. Invest Ophthalmol Vis Sci 51:6784–6792. doi:10.1167/iovs.09-4730

Roopra A, Qazi R, Schoenike B, Daley TJ, Morrison JF (2004) Localized domains of G9a-mediated histone methylation are required for

silencing of neuronal genes. Mol Cell 14:727–738. doi:10.1016/j.molcel.2004.05.026

Rubel EW, Parks TN, Zirpel L (2004) Assembling, connecting and maintaining the cochlear nucleus. In: Parks TN, Rubel EW, Fay RR, Popper AN (eds) Plasticity of the auditory system. Springer, New York, pp 9–48

Satheesh SV, Kunert K, Ruttiger L, Zuccotti A, Schonig K, Friauf E, Knipper M, Bartsch D, Nothwang HG (2012) Retrocochlear function of the peripheral deafness gene Cacna1d. Hum Mol Genet 21: 3896–3909

Saul SM, Brzezinski JA, Altschuler RA, Shore SE, Rudolph DD, Kabara LL, Halsey KE, Hufnagel RB, Zhou J, Dolan DF, Glaser T (2008) Math5 expression and function in the central auditory system. Mol Cell Neurosci 37:153–169

Schaefer A, Sampath SC, Intrator A, Min A, Gertler TS, Surmeier DJ, Tarakhovsky A, Greengard P (2009) Control of cognition and adaptive behavior by the GLP/G9a epigenetic suppressor complex. Neuron 64:678–691. doi:10.1016/j.neuron.2009.11.019

Sharma A, Klein SS, Barboza L, Lohdi N, Toth M (2016) Principles governing DNA methylation during neuronal lineage and subtype specification. J Neurosci 36:1711–1722. doi:10.1523/JNEUROSCI.4037-15.2016

Shi Y (2007) Histone lysine demethylases: emerging roles in development, physiology and disease. Nat Rev Genet 8:829–833. doi:10.1038/nrg2218

Shinkai Y, Tachibana M (2011) H3K9 methyltransferase G9a and the related molecule GLP. Genes Dev 25:781–788. doi:10.1101/gad.2027411

Sun H, Maze I, Dietz DM, Scobie KN, Kennedy PJ, Damez-Werno D, Neve RL, Zachariou V, Shen L, Nestler EJ (2012) Morphine epigenomically regulates behavior through alterations in histone H3 lysine 9 dimethylation in the nucleus accumbens. J Neurosci 32:17454–17464. doi:10.1523/JNEUROSCI.1357-12.2012

Sweatt JD (2013) The emerging field of neuroepigenetics. Neuron 80: 624–632. doi:10.1016/j.neuron.2013.10.023

Tachibana M, Sugimoto K, Nozaki M, Ueda J, Ohta T, Ohki M, Fukuda M, Takeda N, Niida H, Kato H, Shinkai Y (2002) G9a histone methyltransferase plays a dominant role in euchromatic histone H3 lysine 9 methylation and is essential for early embryogenesis. Genes Dev 16:1779–1791. doi:10.1101/gad.989402

Tachibana M, Ueda J, Fukuda M, Takeda N, Ohta T, Iwanari H, Sakihama T, Kodama T, Hamakubo T, Shinkai Y (2005) Histone methyltransferases G9a and GLP form heteromeric complexes and are both crucial for methylation of euchromatin at H3-K9. Genes Dev 19: 815–826. doi:10.1101/gad.1284005

Waddington CH (1942) The epigenotype. Endeavour 1:18–20

Wang HC, Bergles DE (2015) Spontaneous activity in the developing auditory system. Cell Tissue Res 361:65–75. doi:10.1007/s00441-014-2007-5

Wang L, Xu S, Lee J-E, Baldridge A, Grullon S, Peng W, Ge K (2013) Histone H3K9 methyltransferase G9a represses PPARgamma expression and adipogenesis. EMBO J 32:45–59. doi:10.1038/emboj.2012.306

Weiss T, Hergeth S, Zeissler U, Izzo A, Tropberger P, Zee BM, Dundr M, Garcia BA, Daujat S, Schneider R (2010) Histone H1 variant-specific lysine methylation by G9a/KMT1C and Glp1/KMT1D. Epigenetics Chromatin 3:7. doi:10.1186/1756-8935-3-7

Willaredt MA, Ebbers L, Nothwang HG (2014) Central auditory function of deafness genes. Hear Res 312:9–20. doi:10.1016/j.heares.2014.02.004

Yang Z, Ding K, Pan L, Deng M, Gan L (2003) Math5 determines the competence state of retinal ganglion cell progenitors. Dev Biol 264: 240–254

Yao B, Jin P (2014) Unlocking epigenetic codes in neurogenesis. Genes Dev 28:1253–1271. doi:10.1101/gad.241547.114

Yu W-M, Goodrich LV (2014) Morphological and physiological development of auditory synapses. Hear Res 311:3–16. doi:10.1016/j.heares.2014.01.007

Yu H, Lin Q, Wang Y, He Y, Fu S, Jiang H, Yu Y, Sun S, Chen Y, Shou J, Li H (2013) Inhibition of H3K9 methyltransferases G9a/GLP prevents ototoxicity and ongoing hair cell death. Cell Death Dis 4:e506. doi:10.1038/cddis.2013.28

Zhang X, Wen H, Shi X (2012) Lysine methylation: beyond histones. Acta Biochim Biophys Sin 44:14–27. doi:10.1093/abbs/gmr100